Biochemical Synthesis and Manipulation of a 70 nm DNA Linker for the Assembly of DNA-Functionalized Gold Nanoparticles

ARTICLE *in* ADVANCED FUNCTIONAL MATERIALS · JANUARY 2007

Impact Factor: 11.81 · DOI: 10.1002/adfm.200600694

DOI: 10.1002/adfm.200600694

Biochemical Synthesis and Manipulation of a 70 nm DNA Linker for the Assembly of DNA-Functionalized Gold Nanoparticles**

By *Pompi Hazarika*, *Jessica Irrgang*, *Mark Spengler*, and *Christof M. Niemeyer**

DNA oligonucleotides are extraordinarily well suited as linkers for the programmable assembly of nanoparticles. To extend the scope of DNA-directed particle assembly, a 70 nm DNA linker molecule for the DNA-directed assembly of gold nanoparticles is synthesized by biochemical reactions. In particular, polymerase chain reaction (PCR) and subsequent restriction and ligation reactions are employed to synthesize the DNA linker, comprising a 178 base pair (bp) double helical core region supplemented with two sticky-end binding sites of 12 nucleotides in length, attached to one of the core-forming strands. The linker is used for the assembly of DNA-functionalized gold nanoparticles employing yet another biochemical reaction, namely covalent linkage through the enzyme DNA ligase. The resulting nanoparticle assemblies are characterized by using atomic force microscopy. The methodology described here represents a general way of synthesizing programmable DNA linker molecules with dimensions that exceed those presently available by using chemical synthetic methods, and thus, supplements the synthetic toolbox of nanobiotechnology to asses complex and functional nanoparticle/linker architectures for potential applications in sensing and materials science.

1. Introduction

Since its initial description by the groups of Mirkin[1] and Alivisatos,[2] the DNA-directed assembly of semiconductor and metal nanoparticles has gained increasing attention, owing to a broad scope of applications ranging from bioanalytics to materials synthesis.[3–9] With respect to the latter, efforts have been undertaken to specifically tailor DNA linker molecules that contain single-stranded sticky ends capable of hybridizing to their complementary oligomer counterparts immobilized at the particles to be aggregated, such as DNA-modified gold nanoparticles (DNA–AuNPs, see Fig. 1). For example, functional DNA moieties comprising distinct secondary structure elements were incorporated into the linker sequence to add catalytic functionality of DNAzymes to oligomeric DNA–AuNP aggregates,[10–13] and DNA linkers containing single-stranded dangling end overhangs were used for the reversible switching of DNA–AuNP aggregation.[14] Moreover, many fundamental studies, for instance, the investigation of the effects of linker length on the assembly kinetics of DNA–AuNPs,[15] require the availability of DNA linker molecules that comprise two single-stranded sticky ends, typically about 12 nucleotides (NTs) in length, tethered to the 3′ and 5′ end of a double-stranded core region (Fig. 1). Usually, such linker molecules are synthesized by using solid-phase phosphoramidite chemistry. However, because chemical oligonucleotide synthesis currently reaches its limits at oligomer lengths of about 130 NTs (corresponding to about 45 nm length), DNA spacer molecules of greater length are not accessible by using this methodology. To circumvent this limitation, we report here on the utilization of biochemical means, including polymerase chain reaction (PCR), enzymatic restriction, and ligation to synthesize a 70 nm DNA linker molecule, suitable for interconnecting DNA–AuNPs by means of specific Watson–Crick hybridization.

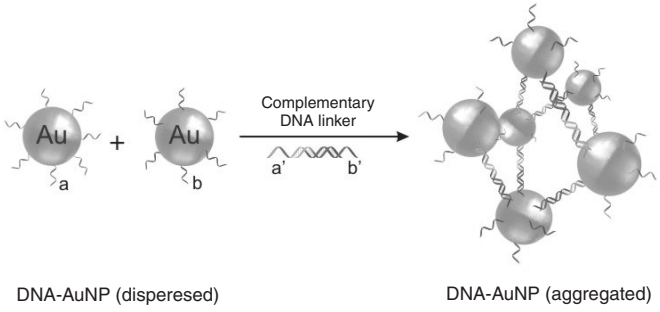

Figure 1. Schematic drawing of DNA-directed assembly of DNA–AuNPs in solution through hybridization with the complementary linker DNA.

2. Results and Discussion

Our synthetic approach is schematically depicted in Figure 2a. It starts with the synthesis of a 192 base pair (bp) dsDNA fragment by using PCR, using the pTyB1 *E. coli* expression cloning vector (7.5 kb) as the template and two pri-

[*] Prof. C. M. Niemeyer, Dr. P. Hazarika, J. Irrgang, M. Spengler
Universität Dortmund, Fachbereich Chemie
Biologisch-Chemische Mikrostrukturtechnik
Otto-Hahn Str. 6, 44227 Dortmund (Germany)
E-mail: christof.niemeyer@uni-dortmund.de

[**] This work was supported by the Zentrum für Angewandte Chemische Genomik, a joint research initiative founded by the European Union and the Ministry of Innovation and Research of the state Northrhine Westfalia.

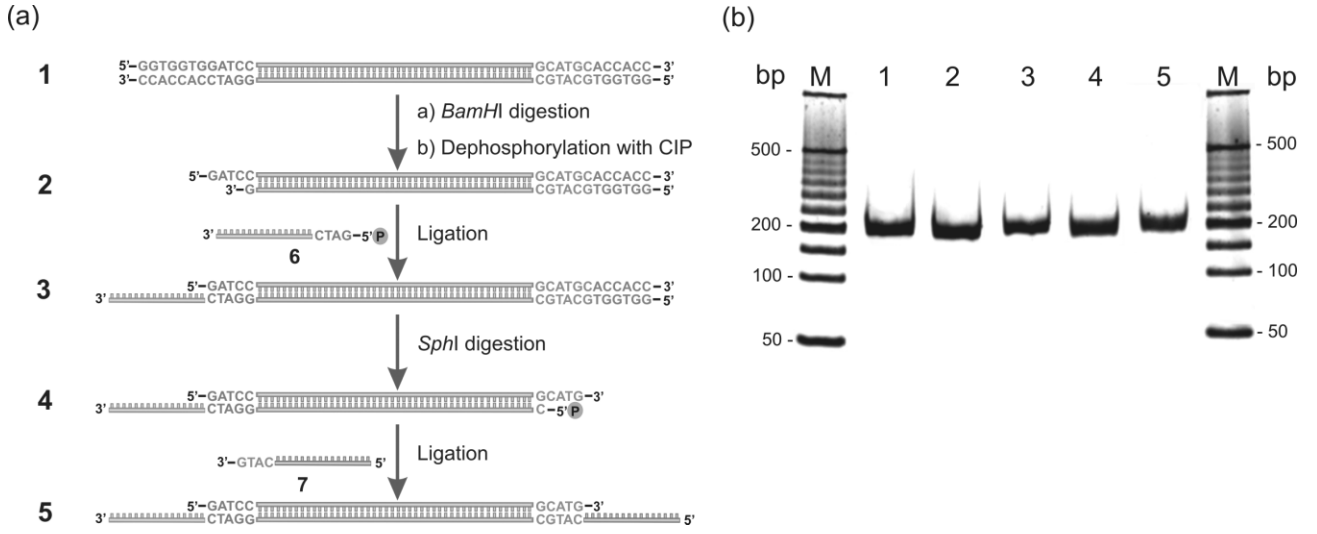

Figure 2. a) Schematic illustration of the synthesis of DNA linker **5**. b) Electrophoretic mobility of the DNA linker (**5**), starting material (**1**) and the intermediate products (**2**–**4**), analyzed on a 15 % nondenaturing polyacrylamide gel stained with SybrGold. Lane 1: PCR product **1** (192 base pairs (bps)); lane 2: *BamH*I digested product **2** (185 bases); lane 3: ligated product **3** (197 bases); lane 4: *Sph*I digested product **4** (190 bases); lane 5: ligated product **5**, that is, the desired DNA linker (202 bases); lanes M contain 50-bp DNA ladders.

mers that contain restriction sites for the enzymes *BamH*I (forward primer) and *Sph*I (reverse primer). The 192-bp PCR product (**1** in Fig. 2a) was then digested with *BamH*I, and to avoid self-ligation in the course of upcoming ligation reactions, the 5′-phosphate group of the resulting sticky ends was dephosphorylated with calf-intestinal alkaline phosphatase (CIP). This led to the restriction product **2**, which contained a 181-bp dsDNA core region and a four NT sticky-end overhang at the 5′ end. Subsequently, a 16 NT synthetic oligonucleotide, **6** in Figure 2a, was ligated to the sticky end of **2**, thereby producing DNA **3**, which now contained the desired 12 NT sticky end at the 5′ end of the dsDNA core of **3**. Molecule **3** was then digested with the enzyme *Sph*I, leading to product **4**, which contained a 3′ overhang of four NTs. Finally, a second 16 NT synthetic oligomer (**7**) was ligated to the sticky end of **4**, thus leading to the desired DNA linker molecule **5**, which contained a double helical core segment of 178 base pairs of which one DNA strand contained the two sticky ends of 12 NT at both of its 5′ and 3′ ends. Starting material **1**, final product **5**, and the intermediate products **2**–**4** were analyzed by using gel electrophoresis, using a 15 % non-denaturing polyacrylamide gel (Fig. 2b). The observed changes in electrophoretic mobility were only small due to the comparably low molecular weights of the restricted and ligated fragments with respect to the 178-bp core region. Nonetheless, the gradual increase (steps **1**→**2** and **3**→**4**) and decrease (steps **2**→**3** and **4**→**5**), respectively, in electrophoretic mobility were distinguishable in the gel image, and thus, provided initial evidence for the successful biochemical synthesis of linker molecule **5**.

To further investigate the integrity and functionality of linker **5**, a solid-phase hybridization assay was carried out (Fig. 3). To this end, streptavidin (STV; a homotetrameric protein) coated microtiter plates were functionalized with biotinylated capture oligomers **8**, which are complementary to the 5′-overhang of linker **5**. Linker **5** was then allowed to hybridize to the surface-bound capture oligomers and the plate was washed to remove unbound materials. To detect immobilized linker **5**, we used the DNA–protein conjugate **9**, which was assembled from a respective covalent DNA–STV adduct, bearing the 12-mer oligonucleotide complementary to the 3′ overhang of **5**, and biotinylated alkaline phosphatase, prepared as previously described through biotin–STV interaction.[16,17] Following the incubation of **9**, the plate was washed again, and Attophos was added as the fluorogenic substrate for the alkaline phosphatase. The fluorescence intensities observed (Fig. 3b) clearly indicated that linker **5** was capable of immobilizing conjugate **9** at the microplate's surface. Negative control reactions, carried out in the absence of **5** (NC 1 in Fig. 3b) or using the noncomplementary DNA–STV–AP conjugate **10** (NC 2), showed only very weak signal intensities comparable to the background signal (blank) where no linker and DNA–STV–AP conjugate were added. This confirmed that linker **5** showed the expected hybridization capabilities and specificity.

To estimate the hybridization efficiency of **5**, further solid-phase binding assays were carried out by using linker **11**, which was simply a single-stranded 24-mer oligonucleotide capable of bridging capture oligomer **8** and conjugate **9**. The resulting fluorescence signals of this assay, shown in Figure 3c, indicate that linker **5** provided an approximate 9-fold reduced hybridization efficiency, compared to the direct linkage through **11**. This result is in agreement with earlier work of Mirkin and coworkers,[15] who showed that longer linkers, containing up to 48-bp dsDNA core regions, significantly slow down the kinetics of hybridization-based DNA–AuNP assembly.

We then investigated the use of linker **5** to aggregate DNA–AuNPs, according to the scheme shown in Figure 1. To this end, DNA–AuNPs **12** and **13** were used bearing oligonucleotides complementary to the sticky ends of **5**. Following the pro-

ADVANCED FUNCTIONAL MATERIALS

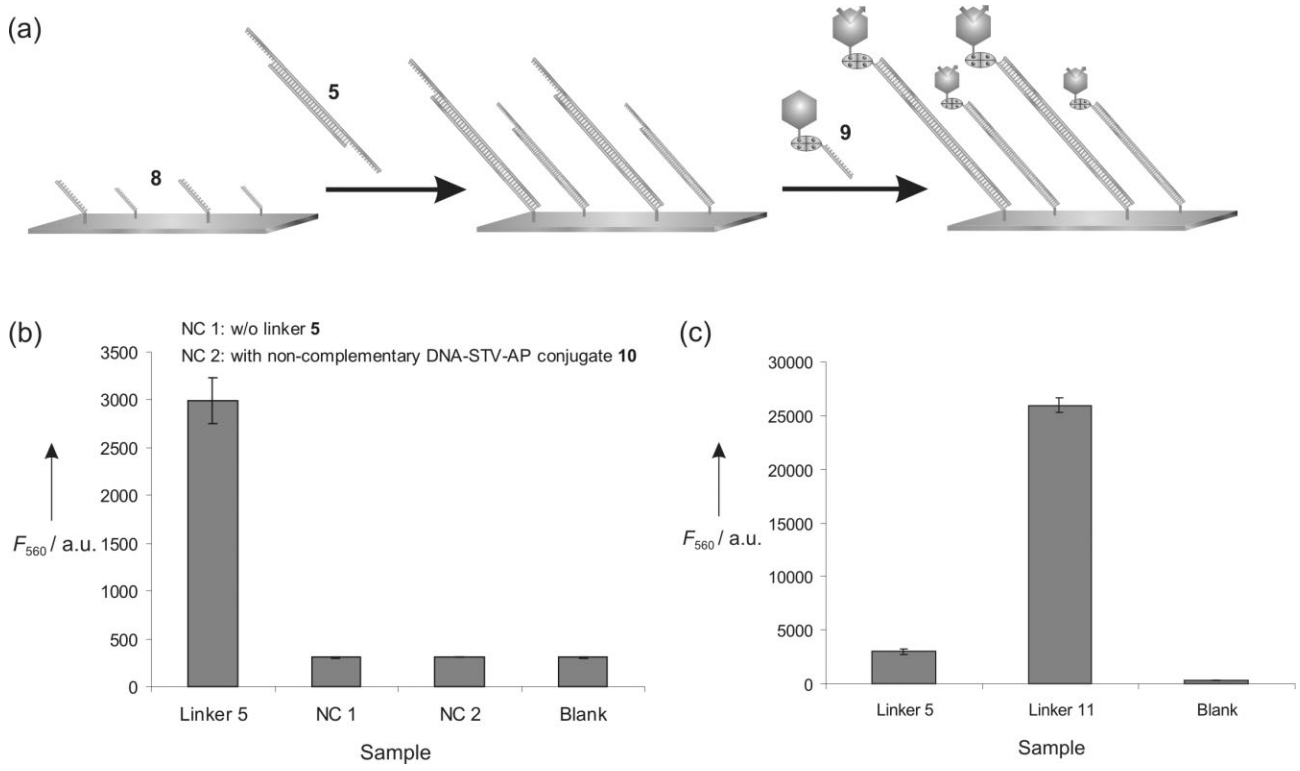

Figure 3. a) DNA-directed immobilization (DDI) of the DNA linker **5** in microtiter plates (MTPs). In the first step, biotinylated capture oligonucleotides **8** were immobilized on STV-coated microplate, then linker **5** was immobilized, and subsequently, complementary DNA–STV hybrid coupled with biotinylated AP (**9**) was immobilized by DNA hybridization. The signal intensities of the assay were obtained using fluorescence spectroscopy (λ_{Exc} = 420 nm, λ_{Emm} = 560 nm). b,c) Fluorescence emission intensities of the solid-phase hybridization assay obtained by using Attophos Substrate (λ_{Exc} = 420 nm, λ_{Emm} = 560 nm). b) Signal intensity of the linker **5** along with the signals for controls, without linker (NC 1) and with noncomplementary DNA–protein conjugate **10** (NC 2). c) The hybridization signal of linker **5** is compared with that of the short linker oligomer **11**.

tocols established for DNA-directed particle aggregation,[14,18] 16 molar equivalents of linker **5** were mixed with one equivalent each of the DNA–AuNPs **12** and **13**, and the mixture was incubated for about 24 h at room temperature. Naked-eye inspection did not indicate the formation of macroscopic AuNP aggregation, and therefore, the sample was analyzed by using atomic force microscopy (AFM). To this end, mica substrates pretreated with $MgCl_2$ were used to immobilize the DNA–AuNPs. As shown in Figure 4, the AFM images only revealed randomly distributed and dispersed particles. This suggests that the DNA–AuNPs were not crosslinked through the linker, likely due to the low hybridization efficiency of the linker, previously observed in the solid-phase hybridization assay (Fig. 3).

We then investigated whether the crosslinking of the DNA–AuNPs might be stabilized by covalent linkage through a ligation reaction using the enzyme DNA ligase. Because this enzymatic reaction requires a 5′-phosphate group at the oligonucleotide to be ligated,[19] we prepared DNA–AuNPs **14** using an oligonucleotide with the identical sequence of **12** but, in addition to the 3′-thiol modification, bearing a 5′-phosphate group to enable covalent linkage with the linker **5** by means of DNA ligase. Moreover, to enable ligation of **5** with the free 3′-hydroxyl group of the oligonucleotides attached to AuNPs **13**, an aliquot of linker **5** was treated with the enzyme T4 polynucleotide kinase and adenosine triphosphate (ATP). This reaction specifically introduces a phosphate group at the 5′-terminus of polynucleotides,[19], that is, the linker molecule **5**. The 5′-phosphorylated linker was added to the mixture of the DNA–AuNPs **14** and **13** along with the enzyme T4 DNA ligase, to enable the covalent ligation reaction between the AuNP-bound DNA oligonucleotides and linker **5**. As a control, we also prepared a similar sample containing all the above-mentioned reagents except the DNA linker **5**.

Subsequent to incubation for about 24 h at 16 °C, the samples were analyzed by using AFM. As shown in Figure 5a, AFM analysis revealed the presence of distinct particle aggregates in the ligation sample (indicated by arrows in Fig. 5a), while no such aggregates were observable in the control sample (Fig. 5b). Owing to the heights of the AuNPs of about 23 nm and associated AFM tip-broadening effects, the DNA linker **5** could not be directly visualized by using AFM (Fig. 5a). The AFM images showed mostly 2D aggregates (Fig. 5a), in which the measured heights of the AuNPs were, on average, 23 nm. To calculate interparticle distances, the very few 3D aggregates, which were indicated by larger heights of the DNA–AuNPs, were not considered. Only interparticle distances in the range of 10–130 nm were taken into account (see the zoom-in image and cross-sectional profile of a typical distance measurement in Fig. 5c). The plot of typical center-to-center distances measured in particle aggregates (Fig. 5a and c) led to a median val-

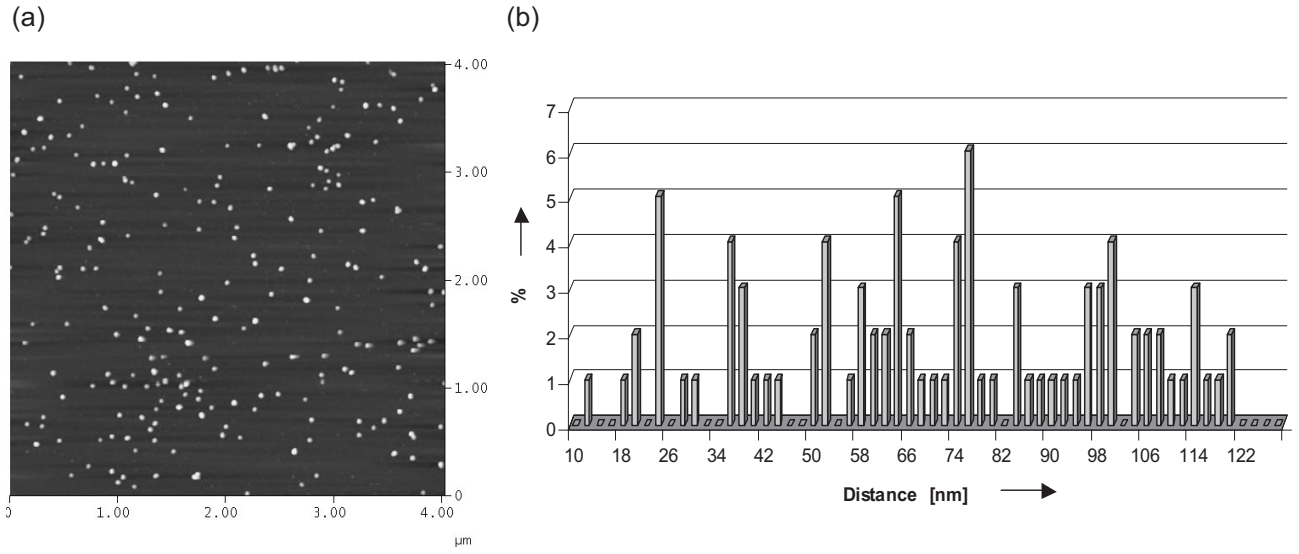

Figure 4. a) AFM image of the sample containing **12** and **13** along with the linker **5**; b) percentage occurrence of interparticle distances. The interparticle spacings were determined from the images by software section analysis of at least 100 particles revealing interparticle spacings in the range of 10–130 nm.

ue of about 86 nm (Fig. 5d). In contrast, similar measurements of the control sample lacking linker **5** showed only randomly distributed dispersed particles (Fig. 5b and d). By subtracting the average particle diameter (ca. 23 nm) from a value of 86 nm, determined from Figure 5a, the apparent linker length was calculated to be ca. 63 nm. Under the assumption that the linker adopts a B-DNA conformation (0.34 nm per bp), this value corresponded well with the theoretically calculated value of 68.7 nm. The observed difference between the calculated and the theoretical values of about 6 nm is likely to be caused by nonlinear, for example, kinked conformations of the linker. Because the length of **5** exceeds the persistence length of dsDNA (ca. 50 nm) it is flexible, and thus, can adopt various different conformations.

3. Conclusions

We have shown an example of how to use biochemical methods for the synthesis of DNA molecules of distinct lengths and tailorable binding properties. In particular, we used PCR and subsequent restriction and ligation reactions to synthesize DNA linker molecules of ca. 70 nm in length, comprising a 178-bp double helical core region containing two sticky-end binding sites of 12 NTs, attached to one of the core-forming strands. We demonstrated the linker's functionality, that is, its capability to specifically hybridize with complementary DNA stretches, bound to either planar surfaces of a microplate or to the curved surface of AuNPs. Moreover, we demonstrated that this linker was susceptible to further biochemical manipulations, in particular, the enzyme mediated covalent ligation with DNA-functionalized AuNPs. Since the biochemical methods used here are amenable to other DNA molecules as well, our approach of linker synthesis represents a general way of producing tailored, and thus, programmable DNA linker molecules of dimensions that exceed those presently available from using chemical synthetic methods. Although this long linker revealed lower hybridization efficiency than short oligonucleotides, we anticipate that the extensive use of biochemical methodology enriches the toolbox of nanobiotechnology and will open the door to more complex and functional nanoparticle/linker architectures, comprising, for instance, recognition sites for enzymatic cleavage or transcription. This may lead to advanced applications in sensing and materials production.

4. Experimental

For the synthesis of DNA linker **5**, a 192-bp dsDNA fragment was generated by using PCR using pTyB1 *E. coli.* expression cloning vector for C-terminal fusion of intein tag (75 kB; New England Biolabs). The forward (5′-GGT GGT GGA TCC AGG GGA ATT GTG AGC GGA TAA CAA T-3′) and reverse (5′-GGT GGT GCA TGC AAT AGA CCC ATC CGC CAT TAA AAC A-3′) primers used for PCR were purchased from Thermo Electron. PCR products were purified by non-denaturing agarose gel electrophoresis using a commercial gel extraction kit (UltraPrep Gel-Ex; Molzym). The first enzymatic digestion step was carried out by incubating the PCR product **1** (75 pmol) with 60 units of *BamH*I (New England Biolabs) for 2 h at 37 °C in NEB(2) (i.e., 50 mM NaCl, 10 mM Tris-HCl, 10 mM $MgCl_2$, 1 mM Diothiothreitol, pH 7 at 25 °C) buffer (New England Biolabs). Following, the *BamH*I digested DNA was treated with 10 units of CIP for 1 h at 37 °C, to dephosphorylate the 5′ ends of the digested products. The first enzymatic ligation reaction was carried out by incubating product **2** (52 pmol) with 50 molar equivalents of **6** (5′-phosphate-GAT CGA TCT CTT CAC C-3′) and 400 units of T4 DNA ligase (New England Biolabs) in a buffer containing 50 mM Tris-HCl, 10 mM $MgCl_2$, 1 mM ATP, 10 mM DTT, 25 µg mL^{-1} BSA (pH 7.5), for 30 min at 16 °C. The second enzymatic digestion step was carried out by incubating product **3** (36 pmol) with 20 units of *Sph*I (New England Biolabs) for 2 h at 37 °C in NEB(2) buffer(New England Biolabs). The second enzymatic ligation step was carried out similarly as the first ligation step by incu-

ADVANCED FUNCTIONAL MATERIALS

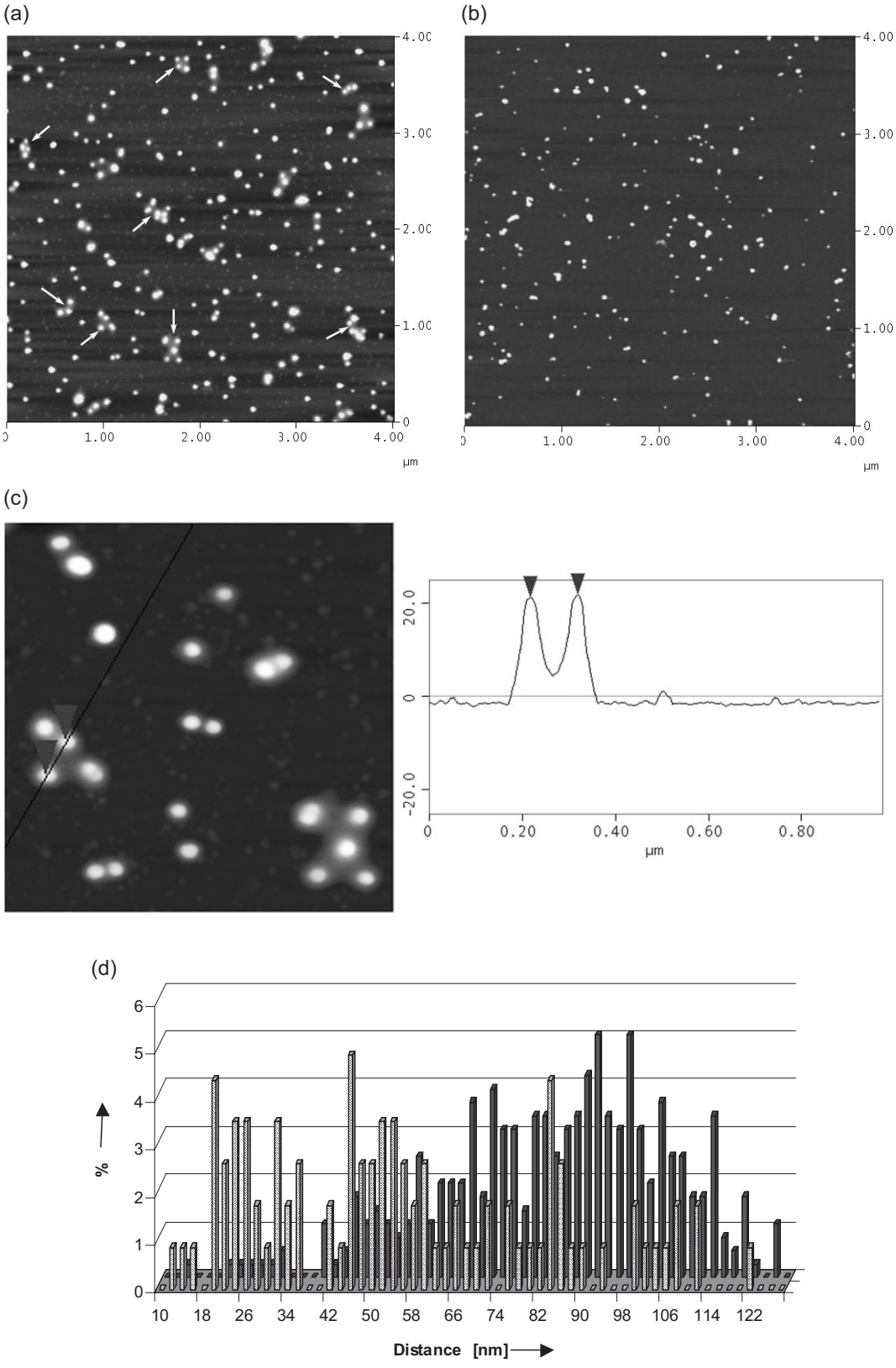

Figure 5. AFM images of a) assembled DNA–AuNPs (some typical particle assemblies are indicated by arrows), and b) the control reaction without linker; c) zoom-in image of Figure 5a and cross-sectional profile of a typical interparticle distance measurement; d) relative percentage occurrence of the interparticle distances with (grey bars) and without (dashed bars) the linker **5**. The interparticle spacings were determined from the images by software section analysis of about 350 particles revealing interparticle spacings in the range of 10–130 nm.

bating product **4** (23 pmol) with 50 molar equivalents of **7** (5′-CAG GAT GGT CTT CAT G-3′) and 400 units of T4 DNA ligase (New England Biolabs).

The polyacrylamide gel electrophoresis (PAGE) was carried out using a 15 % non-denaturing polyacrylamide gel. The electrophoresis was performed in TBE buffer (89 mM Tris-HCl, 89 mM boric acid, 2 mM EDTA, pH 8.4) (EDTA: ehhylene diamine tetraacetic acid) for 1 h at 150 V. The gel was stained with the intercalating dye SybrGold (Molecular Probes), and bands were visualized and photographed under UV light using a gel documentation device (AlphaImager, Alpha Innotech).

For the DDI experiment, the microplate was functionalized with STV as previously described [16]. 50 μL of a 240 nM solution of the biotinylated capture oligonucleotides **8** (5′-AAG ACC ATC CTG TTT TTT TTT TTT-Biotin-3′) in TETBS buffer (i.e., 20 mM Tris-HCl, 150 mM NaCl, 5 mM EDTA, 0.05 % Tween-20, pH 7.35) was incubated in each well of the STV-coated microplate for 30 min at room temperature. The unbound oligonucleotides were removed by washing the plate with TETBS four times (twice for 30 s, twice for 5 min). Subsequently, 50 μL of a 200 nM solution of each of linker DNA, either **5** or **11** (5′-CAG GAT GGT CTT GAT CTC TTC ACC-3′), in TETBS buffer containing 300 mM NaCl were allowed to bind to the immobilized capture DNA in separate wells of the microplate for 30 min at room temperature. The excess DNA linkers were removed by washing the plate as described above. Following, 50 μL (100 nM) of conjugate **9** were added to each well containing the immobilized linker DNA and incubated for 45 min at room temperature. **9** was prepared by covalent synthesis from STV and a thiolated oligonucleotide (5′-Thiol-GGT GAA GAG ATC-3′) complementary to the 3′ overhang of **5**, and subsequently coupled with biotinylated alkaline phosphatase, as previously described [20]. After the incubation period, the microplate was washed again to remove excess reagents. The read-out signals were generated by adding 50 μL of AttoPhos solution to each microwell and the signals were measured after an incubation period of 30 min with a Synergy HT microtiter plate reader (Bio-Tek), using excitation and emission wavelengths of 420 and 560 nm, respectively. The control experiments were also carried out similarly by incubating all reagents in the absence of the linker DNA, and by using noncomplementary DNA–STV conjugate **10**, containing oligonucleotide 5′-thiol-GTA ATC ATG GTC ATA GCT GTT-3′.

For studying the assembly of AuNPs, DNA–AuNPs were synthesized as previously described using 22.9 ± 5.7 nm citrate-stabilized gold nanoparticles [14,18,21]. For the first hybridization experiment, 15 fmol (3 nM) of conjugate **12** (AuNP containing oligomer 5′-AAG ACC ATC CTG-Thiol-3′) were mixed with 15 fmol (3 nM) of conjugate **13** (AuNP containing oligomer 5′-thiol-GGT GAA GAG ATC-3′) and then 16 molar equivalents (7 μL, 69 nM) of the linker DNA **5** were added. The mixture was incubated overnight at room temperature and subsequently analyzed by using AFM. For the second hybridization experiment, the DNA–AuNPs **14** (AuNP containing oligomer 5′-Phosphate-AAG ACC ATC CTG-Thiol-3′) and **13** were used. To phosphorylate the DNA linker **5**, it was incubated with 25 units of T4 polynucleotide kinase (New England Biolabs) in buffer containing 50 mM Tris-HCl, 10 mM $MgCl_2$, 1 mM ATP (pH 7.5), and the mixture was incubated for 30 min at 37 °C. To carry out the ligation reaction with DNA–AuNPs, 15 fmol of conjugate **14** (3 nM) were mixed with 15 fmol of conjugate **13** (3 nM) and then 16 molar equivalents of the phosphorylated linker **5** were added. Subsequently, 800 units of T4 DNA ligase was added, and the mixture was incubated overnight at 16 °C. The negative control sample was prepared in a similar way using all the above-mentioned reagents, except the DNA linker. The samples were analyzed by using AFM as described below.

To carry out the AFM studies, freshly cleaved muscovite mica was used as the substrate, which was modified with a solution of 10 mM $MgCl_2$ for 45 min. Following this, 10 μL of the sample solution was incubated for 30 min on the magnesium modified mica substrate and excess sample was washed off with water. The mica substrate was dried in a stream of nitrogen. AFM measurements were performed using a NanoWizard (JPK Instruments; Berlin, Germany) mounted on a Zeiss Axiovert 200M (Carl Zeiss; Goettingen, Germany) or a MultiMode SPM microscope equipped with a Nanoscope IIIa Controller (Digital Instruments; Santa Barbara, CA). The microscope was coupled to an AS-12 E-scanner and an Extender Electronics Module EX-II (Digital Instruments; Santa Barbara, CA). Silicon cantilevers PPP-NCHR (nominal spring constant of 42 $N\,m^{-1}$; length of 125 μm; resonance frequency ca. 300 kHz; nominal tip radius of < 10 nm) (Nanosensors; Neuchatel, Switzerland) were used for measurements. AFM measurements were performed using tapping-in-air mode. Scan rates varied from 0.5 to 1.0 Hz, and an amplitude of 2 V was used. The resulting amplitude set point was adjusted to minimal forces. Interparticle spacings were determined by using the free ware WsXM 4.0, Nanotec Electronica SL. For this measurement, particles within close proximity (10–130 nm) and a height of about 23 nm were considered. The cross-sectional profile of a typical interparticle distance measurement (Fig. 5b was recorded using the Nanoscope IV SPM software, Version 5.12r3, Veeco Instruments, Santa Barbara).

Received: August 1, 2006
Revised: October 4, 2006

[1] C. A. Mirkin, R. L. Letsinger, R. C. Mucic, J. J. Storhoff, *Nature* **1996**, *382*, 607.
[2] A. P. Alivisatos, K. P. Johnsson, X. Peng, T. E. Wilson, C. J. Loweth, M. P. Bruchez, Jr., P. G. Schultz, *Nature* **1996**, *382*, 609.
[3] J. J. Storhoff, C. A. Mirkin, *Chem. Rev.* **1999**, *99*, 1849.
[4] C. M. Niemeyer, *Angew. Chem. Int. Ed.* **2001**, *40*, 4128; *Angew. Chem.* **2001**, *113*, 4254.
[5] M. C. Daniel, D. Astruc, *Chem. Rev.* **2004**, *104*, 293.
[6] C. M. Niemeyer, C. A. Mirkin, *NanoBiotechnology: Concepts, Methods and Applications*, Wiley-VCH, Weinheim, Germany **2004**.
[7] E. Katz, I. Willner, *Angew. Chem. Int. Ed.* **2004**, *43*, 6042.
[8] N. L. Rosi, C. A. Mirkin, *Chem. Rev.* **2005**, *105*, 1547.
[9] C. M. Niemeyer, U. Simon, *Eur. J. Inorg. Chem.* **2005**, 3641.
[10] J. Liu, Y. Lu, *J. Fluoresc.* **2004**, *14*, 343.
[11] J. Liu, Y. Lu, *J. Am. Chem. Soc.* **2004**, *126*, 12 298.
[12] V. Pavlov, Y. Xiao, R. Gill, A. Dishon, M. Kotler, I. Willner, *Anal. Chem.* **2004**, *76*, 2152.
[13] J. Liu, Y. Lu, *Anal. Chem.* **2004**, *76*, 1627.
[14] P. Hazarika, B. Ceyhan, C. M. Niemeyer, *Angew. Chem. Int. Ed.* **2004**, *43*, 6469; *Angew. Chem.* **2004**, *116*, 6631.
[15] J. J. Storhoff, A. A. Lazarides, R. C. Mucic, C. A. Mirkin, R. L. Letsinger, G. C. Schatz, *J. Am. Chem. Soc.* **2000**, *122*, 4640.
[16] C. M. Niemeyer, W. Bürger, R. M. J. Hoedemakers, *Bioconjugate Chem.* **1998**, *9*, 168.
[17] U. Feldkamp, R. Wacker, W. Banzhaf, C. M. Niemeyer, *ChemPhysChem* **2004**, *5*, 367.
[18] C. M. Niemeyer, B. Ceyhan, P. Hazarika, *Angew. Chem. Int. Ed.* **2003**, *42*, 5766; *Angew. Chem.* **2003**, *115*, 5944.
[19] F. M. Ausubel, R. Brent, R. E. Kingston, D. D. Moore, J. G. Seidman, J. A. Smith, K. Struhl, *Current Protocols in Molecular Biology*, John Wiley & Sons Inc., New York **1994**.
[20] C. M. Niemeyer, T. Sano, C. L. Smith, C. R. Cantor, *Nucleic Acids Res.* **1994**, *22*, 5530.
[21] P. Hazarika, T. Giorgi, M. Reibner, B. Ceyhan, C. M. Niemeyer, in *Bioconjugation Protocols: Strategies and Methods* (Ed: C. M. Niemeyer), Humana Press, Totowa, NJ **2004**, p. 295.